Electronic Supplementary Information

New Insights into the Multi-Step Reaction Pathway of the Reductive Half-Reaction Catalysed by Aromatic Amine Dehydrogenase: A QM/MM Study

Jiayun Pang,[†,‡] Nigel S. Scrutton,[†,§] Sam P. de Visser,[†,‡] and Michael J. Sutcliffe*[,†,‡]

[†]Manchester Interdisciplinary Biocentre, [‡]School of Chemical Engineering and Analytical Science, [§]Faculty of Life Sciences, University of Manchester, 131 Princess Street, Manchester M1 7DN, UK

1. Computational Details

Setup of molecular dynamics (MD) simulations

AADH adopts an $\alpha_2\beta_2$ heterotetrametic structure, where the α subunit has a molecular mass of 40 kDa and the TTQ-containing β subunit a mass of 14 kDa (Figure S1(A)). The TTQ cofactor is formed by post-translational modification of two gene-coded tryptophan residues (Trp 109 and Trp 160) and is tightly associated with the backbone of the rest of the enzyme structure via hydrogen bonds (Figure S1(B)). Crystal structures of the tryptamine-AADH intermediate complexes have been solved for intermediates V and VII (PDB accession codes 2AGY and 2AGZ, respectively).[1] We first performed molecular dynamics (MD) simulations of intermediates III (modelled based on V and the structural information obtained by using inhibitor phenylhydrazine as substrate[1]) and VII. The atom types and the corresponding force constants to describe the tryptamine-bound TTQ were assigned by analogy with similar chemical moieties and also based on a previous study of MADH.[2] The

equilibrium values for the bonds, angles and dihedral angles were obtained by optimising tryptamine-bound TTQ using B3LYP/6-31G* level of theory. The partial atomic charge for the substrate was computed by RED [3] in conjunction with RESP implemented in AMBER9.[4]

The full tetrameric structure of AADH (Figure S1(A)) was solvated in a truncated octahedral water box using the TIP3P model with 8 Å between the edge of the box and the protein. The protonation state of the ionizable residues was determined at *p*H 7 using H++ (http://biophysics.cs.vt.edu/H++),[5,6] a web-based system that computes *p*K values of ionizable groups in enzymes. Four Na^+ ions were added to neutralize the net charge of the system of intermediate III and VII, respectively. MD simulations were carried out using the AMBER ff96 forcefield[7] in AMBER9.[4] Following minimisation and a 300 ps equilibration, the production trajectory was collected for 1 ns and analyzed for the root-mean-square deviations (RMSDs) and root-mean-square fluctuations (RMSFs) to ensure the overall stability of the trajectories. Three to four snapshots from the MD trajectory were selected randomly for the subsequent QM/MM calculations.

QM/MM potential energy scan

The subsequent QM/MM calculations have been performed with a two-layer ONIOM scheme as implemented in G03,[8] where the interface between the QM and the MM regions is treated by link atoms.[9] A small QM region (45 atoms) was firstly used, consisting of the tryptophyl quinone moiety of the TTQ with tryptamine bound and the carboxylate group of the active site base Asp128β, with 3 link atoms connecting this to the MM region (Figure S1(B)). However, this definition of QM region grossly underestimated the activation energy and overestimated the energy of reaction for the proton transfer reaction in going from intermediate III to IV (see Results and

Discussion; Figure S2). A larger QM definition comprising 104 atoms with 10 link atoms was then applied to incorporate more accurately the electrostatic interactions through hydrogen bonds between the carboxylate group of Asp128β, tryptamine-bound TTQ and the active site residues (Figure S3). Due to the large size of AADH (~900 residues), inclusion of the whole enzyme into the MM region in the QM/MM calculations is beyond our computational resources. Thus, only the TTQ-containing small β subunit and the interface between it and the α subunit were defined as the MM region and are free to move (the active MM region). An additional 5 Å layer of the α subunit outside the active MM region protein and a 5 Å layer of water around the β subunit were defined as MM but were kept frozen to maintain the shape of the interface (Figure S1(A)).

The potential energy scans were performed with geometry optimization at each fixed reaction coordinate along a given reaction path using B3LYP/6-31G* level of theory for the QM region and the AMBER 96 force field for the MM region in the ONIOM scheme. The level of theory and basis set for the QM region adequately describes the geometries of the enzyme-substrate complex compared to the available crystal structures and gives a barrier height of the rate-limiting step in close agreement with the experimental data. The combination of B3LYP and 6-31G* provides a balance between the accuracy of calculations and the computational efficiency, given the size of the QM region and the number of reactive intermediates studied. The minima and the transition state on the potential energy surfaces were characterised by frequency calculations at the same level of theory. For both minima and transition states, further optimisations were carried out with the electronic embedding scheme [10, 11] (as suggested by the G03 manual), then single point energy calculations (B3LYP/6-311++G** for the QM region) were performed on the

optimized structure with electronic embedding scheme to obtain the most accurate energies. The energies discussed in our study are relative electronic energies unless otherwise specified.

References

1. L. Masgrau, A. Roujeinikova, L. O. Johannissen, P. Hothi, J. Basran, K. E. Ranaghan, A. J. Mulholland, M. J. Sutcliffe, N. S. Scrutton and D. Leys, *Science*, 2006, **312**, 237-241.
2. G. Pierdominici-Sottile, J. Echave and J. Palma, *J. Phys. Chem. B*, 2006, **110**, 11592-11599.
3. F.-Y. Dupradeau, C. Cezard, R. Lelong, E. Stanislawiak, J. Pecher, J. C. Delepine and P. Cieplak, *Nucl. Acids Res.*, 2008, **36**, D360-367.
4. D. A. Case, T. E. Cheatham, 3rd, T. Darden, H. Gohlke, R. Luo, J. Merz, K. M., A. Onufriev, C. Simmerling, B. Wang and R. J. Woods, *J. Comp. Chem.*, 2005, **26**, 1668-1688.
5. J. C. Gordon, J. B. Myers, T. Folta, V. Shoja, L. S. Heath and A. Onufriev, *Nucl. Acids Res.*, 2005, **33**, W368-371.
6. R. Anandakrishnan and A. Onufriev, *J. Comp. Biol.*, 2008, **15**, 165-184.
7. W. D. Cornell, P. Cieplak, C. I. Bayly, I. R. Gould, J. Merz, K. M., D. M. Ferguson, D. C. Spellmeyer, T. Fox, J. W. Caldwell and P. A. Kollman, *J. Am. Chem. Soc.*, 1995, **117**, 5179-5197.
8. M. J. Frisch, G. W. Trucks, H. B. Schlegel, G. E. Scuseria, M. A. Robb, J. R. Cheeseman, J. Montgomery, J. A., T. Vreven, K. N. Kudin, J. C. Burant, J. M. Millam, S. S. Iyengar, J. Tomasi, V. Barone, B. Mennucci, M. Cossi, G. Scalmani, N. Rega, G. A. Petersson, H. Nakatsuji, M. Hada, M. Ehara, K. Toyota, R. Fukuda, J. Hasegawa, M. Ishida, T. Nakajima, Y. Honda, O. Kitao, H. Nakai, M. Klene, X. Li, J. E. Knox, H. P. Hratchian, J. B. Cross, V. Bakken, C. Adamo, J. Jaramillo, R. Gomperts, R. E. Stratmann, O. Yazyev, A. J. Austin, R. Cammi, C. Pomelli, J. W. Ochterski, P. Y. Ayala, K. Morokuma, G. A. Voth, P. Salvador, J. J. Dannenberg, V. G. Zakrzewski, S. Dapprich, A. D. Daniels, M. C. Strain, O. Farkas, D. K. Malick, A. D. Rabuck, K. Raghavachari, J. B. Foresman, J. V. Ortiz, Q. Cui, A. G. Baboul, S. Clifford, J. Cioslowski, B. B. Stefanov, G. Liu, A. Liashenko, P. Piskorz, I. Komaromi, R. L. Martin, D. J. Fox, T. Keith, M. A. Al-Laham, C. Y. Peng, A. Nanayakkara, M. Challacombe, P. M. W. Gill, B. Johnson, W. Chen, M. W. Wong, C. Gonzalez and J. A. and Pople, *Gaussian, Inc., Wallingford CT*, (2004).
9. J. F. Martin, A. B. Paul and K. Martin, *J. Comput. Chem.*, 1990, **11**, 700-733.
10. T. Vreven, K. S. Byun, I. Komaromi, S. Dapprich, J. A. Montgomery, K. Morokuma and M. J. Frisch, *J. Chem. Theory Comput.*, 2006, **2**, 815-826.
11. D. Bakowies and W. Thiel, *J. Phys. Chem.*, 1996, **100**, 10580-10594.

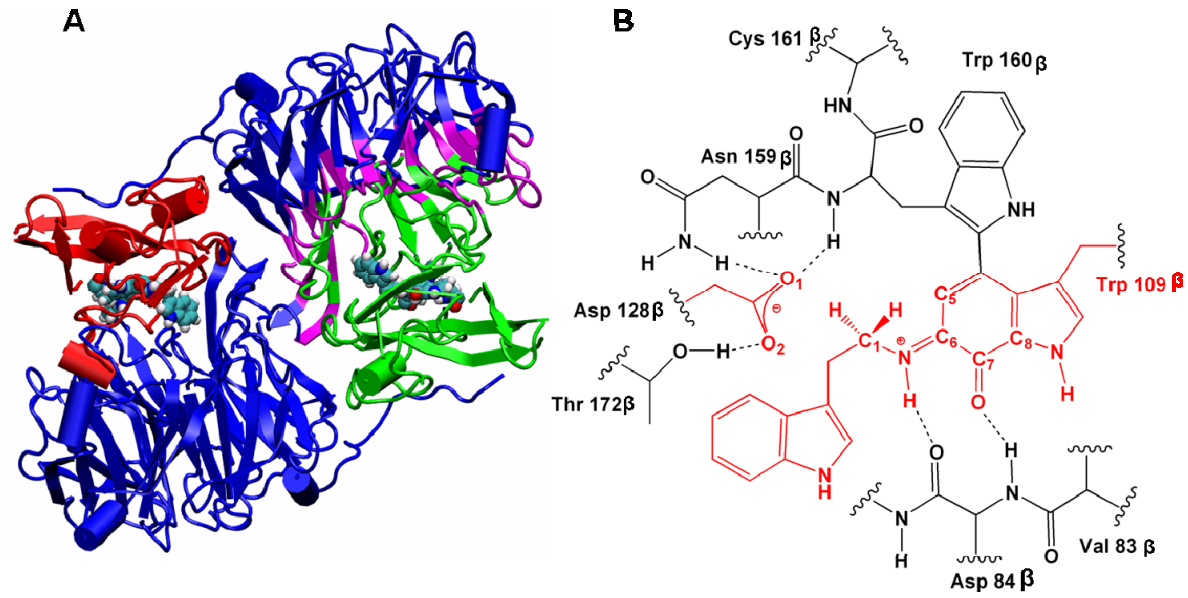

Figure S1: (A) Structure of the TTQ-dependent AADH, with the small subunit depicted in red cartoon, the large subunit in blue cartoon and the TTQ in green spheres in the heterodimer on the left-hand side. In the heterodimer on the right-hand side, the MM atoms free to move in the QM/MM calculations are depicted in green (including the small subunit and the interface between the small and large subunit) and the MM atoms frozen in the QM/MM calculations are depicted in pink. (B) Schematic of the active site of AADH, illustrating the QM definition used in the calculations – the small QM region is depicted in red while the larger 104 atom QM region is depicted in both red and black. The hydrogen bonds are represented by dashed lines.

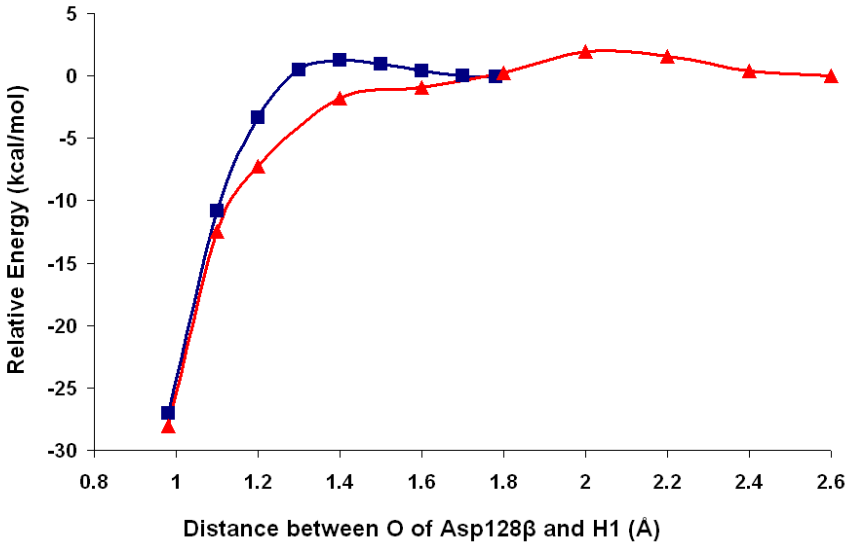

Figure S2: Potential energy surface for the formation of the bond (reactant on the right and product on the left – from intermediate III to IV) between H1 of iminoquinone and O1 (blue squares) and O2 (red triangles) of Asp128β, respectively using the small QM/MM partition of 45 atoms (Figure 1).

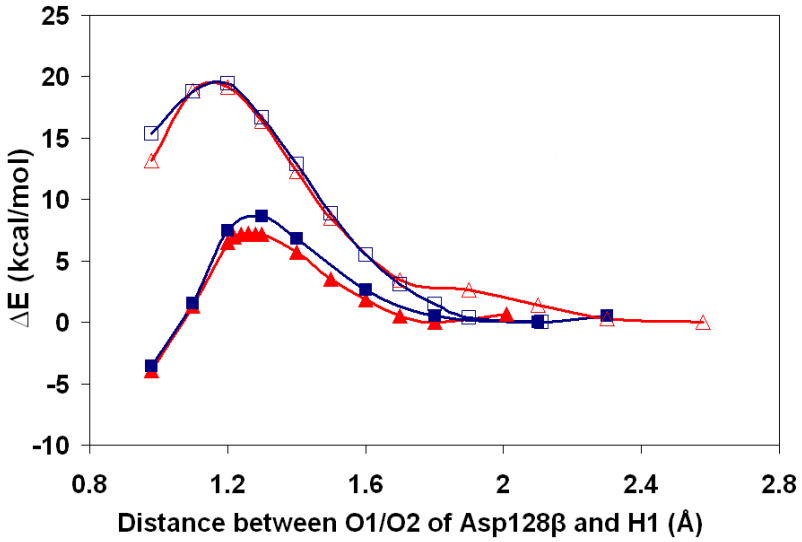

Figure S3. Potential energy surface for the formation of the bond between H1 of iminoquinone and O1 (blue squares) and O2 (red triangles) of Asp128β – from intermediate III to IV – using the QM/MM configuration containing 104 QM atoms (Figure 2B). The solid squares/triangles show the results obtained with mechanical embedding and the open squares/triangles show the results obtained with electronic embedding.

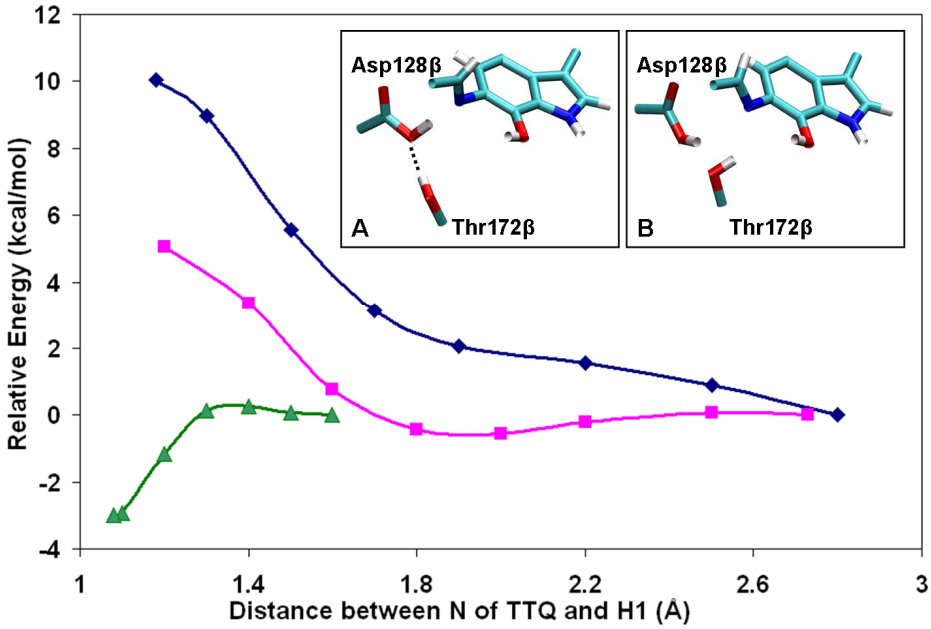

Figure S4: Potential energy surface for the formation of the bond between H1 from O2 of Asp 128 β back to N of the Schiff base – from intermediate V^* to V – obtained using the electronic embedding scheme with B3LYP/6-31G* level of theory for the QM region and the AMBER 96 force field for the MM region (three different starting configurations – blue, magenta and green). The inset illustrates: (A) The configuration where the hydrogen bond remains between O2 of Asp128β and the hydroxyl group of Thr β172. The transfer of H1 is energetically facile (green line in main plot). (B) The configuration where the hydrogen bond is broken with the hydroxyl group of Thr β172 moved away and pointing towards TTQ. The transfer of H1 back to N of the Schiff base is endothermic with a straight energy increase (blue and magenta lines in main plot).

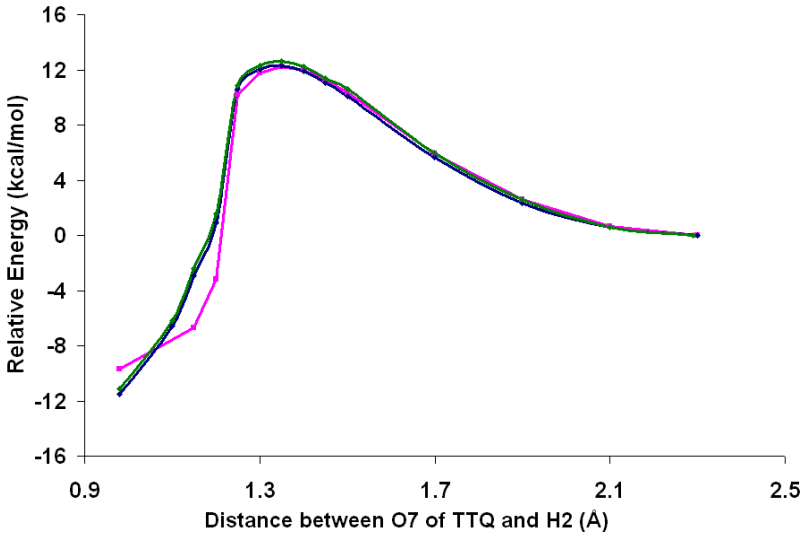

Figure S5: Potential energy surface of the formation of bond between O7 and H2 of iminoquinone, obtained by mechanical embedding scheme using B3LYP/6-31G* level of theory for the QM region and the AMBER 96 force field for the MM region (three different starting configurations (magenta, blue and green)).

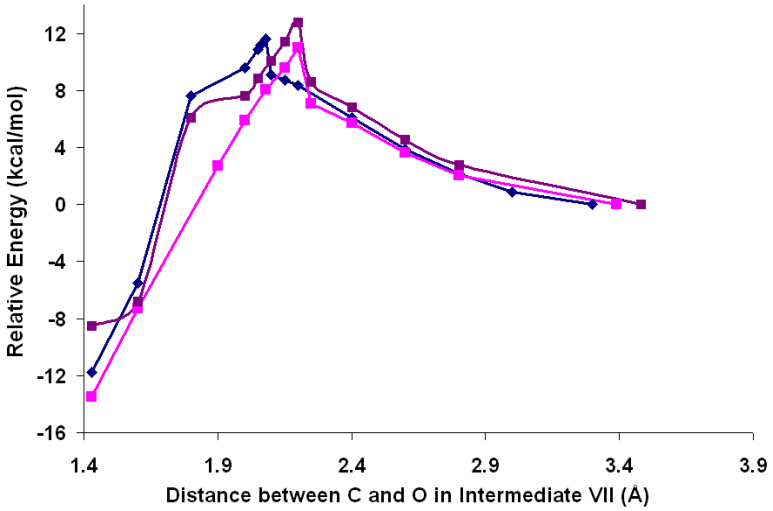

Figure S6: Potential energy surface for the formation of bond between O and C1 – from in intermediate VI to VII – obtained using the mechanical embedding scheme with B3LYP/6-31G* level of theory for the QM region and the AMBER 96 force field for the MM region (three different starting configurations).